

Scalable Primal Decomposition Schemes for Large-Scale Infrastructure Networks

Alexander Engelmann, Sungho Shin,
François Pacaud, and Victor M. Zavala *

December 2, 2024

The operation of large-scale infrastructure networks requires scalable optimization schemes. To guarantee safe system operation, a high degree of feasibility in a small number of iterations is important. Decomposition schemes can help to achieve scalability. In terms of feasibility, however, classical approaches such as the alternating direction method of multipliers (ADMM) often converge slowly. In this work, we present primal decomposition schemes for hierarchically structured strongly convex QPs. These schemes offer high degrees of feasibility in a small number of iterations in combination with global convergence guarantees. We benchmark their performance against the centralized off-the-shelf interior-point solver Ipopt and ADMM on problems with up to 300,000 decision variables and constraints. We find that the proposed approaches solve problems as fast as Ipopt, but with reduced communication and without requiring a full model exchange. Moreover, the proposed schemes achieve a higher accuracy than ADMM.

1. Introduction

The operation of infrastructure networks such as power systems, district heating grids or gas networks is challenging. In many cases, these networks are large and composed of many complex subsystems such as lower-level networks or buildings. Operation is often based on numerical optimization due to its flexibility and recent advances in solver

*This work was supported by the U.S. Department of Energy, Office of Science, Advanced Scientific Computing Research, under contract number DE-AC02-06CH11357. VM Zavala also acknowledges partial support from the U.S. National Science Foundation under award CBET-2315963. This research was conducted while AE was with TU Dortmund University, Dortmund, Germany (alexander.engelmann@ieee.org). SS is with Massachusetts Institute of Technology, Cambridge, MA, USA (sushin@mit.edu). FP is with Centre Mathématiques et Systèmes, Mines Paris-PSL, Paris, France (francois.pacaud@minesparis.psl.eu). VZ is with University of Wisconsin-Madison, Madison, WI, USA and Argonne National Laboratory, Lemont, IL, USA (victor.zavala@wisc.edu).

development, which allows to solve large-scale problems quickly and to a high accuracy. For large networks, however, a centralized solution is often not desirable since, a), the problem becomes computationally challenging, even with state-of-the-art solvers; b), information collection in a central entity should be avoided due to confidentiality and privacy concerns, and, c), the responsibility for operation and updates in modeling should stay mainly in the subsystems.

One line of research addresses the above challenges via aggregation. Here, the idea is to simplify the subproblems by projecting the constraint set on the coupling variables of the infrastructure network. Examples for this can be found for power systems [1, 2]. A drawback of this approach is a loss of optimality. Moreover, aggregation is often not straightforward, feasibility is hard to guarantee and disaggregation requires solving additional local optimization problems.

A second line of research is based on distributed optimization. Prominent approaches are primal and dual first-order algorithms such as Lagrangian dual decomposition, the Alternating Direction Method of Multipliers (ADMM) [3, 4], and primal (sub)-gradient-based schemes [5, 6]. Application examples range from the operation of power systems [7, 8], over gas networks [9], district heating systems [10, 11], to water networks [12]. With their at most linear rate of convergence, these approaches often require many iterations to converge even for a modest solution quality. This is often prohibitive for real-time implementation.

Distributed second-order methods exhibit faster convergence. Here, classical approaches aim at decomposing the block-structure of the Karush-Kuhn-Tucker (KKT) system within interior-point algorithms [13, 14] or sequential quadratic programming [15]. Alternative second-order methods based on augmented Lagrangians can be found in [16, 17]. These approaches typically require an expensive central coordination, although it is possible to partially alleviate computation by decentralizing the Newton-steps [18–20].

Primal decomposition schemes come with the advantage a high degree of feasibility and optimality in a small number of iterations [21–23]. For achieving this, they require a hierarchical problem structure, i.e. a star as the underlying graph. In this sense, they are more restrictive than the aforementioned approaches. In infrastructure networks hierarchical problem structures are common, however. The main idea of primal decomposition is to construct lower-level problems coordinated by one upper-level problem, where the upper-level problem considers the lower-level problems by their optimal value functions. Primal decomposition has been very successful in solving large-scale problems from chemical engineering [24, 25] and some of the largest Quadratic Programs (QPs) and Nonlinear Programs (NLPs) from power systems [26–28]. Moreover, primal decomposition allows to use specialized, domain-specific solvers to solve the subproblems and the master problem efficiently [22].

In this work, we propose two primal decomposition schemes for solving large-scale strongly convex QPs, with global convergence guarantees. Both methods rely respectively on augmented Lagrangians and exact ℓ_1 -penalties for ensuring feasibility in the subproblems. Similar ℓ_1 -penalty based approaches have been proposed in previous works [22, 26]. In contrast to [26], our work is not restricted to a specific application and can be

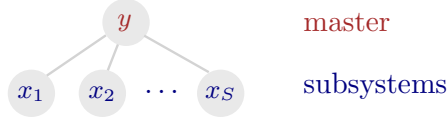


Figure 1: Star graph of problem (1).

used on any strongly convex hierarchically structured QP. The augmented-Lagrangian framework is new to the best of our knowledge. We show that the augmented Lagrangian formulation exhibits improved performance compared to the ℓ_1 formulation. Moreover, we demonstrate that the algorithms are faster than off-the-shelf interior-point solvers. We benchmark our algorithms against a distributed ADMM and the nonlinear solver **Ipopt**. As benchmarks, we consider the operation of HVAC systems in a city district with a variable number of buildings and with up to 300,000 decision variables and inequality constraints and two Optimal Power Flow problems with up to 7,852 buses.

Notation

Given $A \in \mathbb{R}^{m \times n}$, $[A]_j$ denotes the j th row of A and $\text{nr}(A) \doteq m$ corresponds to the number of rows of A . The Lagrange multiplier $\lambda \in \mathbb{R}^{n_g}$ associated to a constraint $g : \mathbb{R}^{n_x} \rightarrow \mathbb{R}^{n_g}$ is written as $g(x) = 0 \mid \lambda$. Given a vector $v \in \mathbb{R}^n$, $D = \text{diag}(v) \in \mathbb{R}^{n \times n}$ denotes a matrix with the elements of v on the main diagonal. For a tuple of matrices (A, B) , $\text{blkdiag}(A, B)$ denotes their block-diagonal concatenation.

2. Problem Formulation

Many infrastructure network problems can be formulated as strongly convex QPs over a set of subsystems $\mathcal{S} = \{1, \dots, S\}$,

$$\min_{\{x_i\}_{i \in \mathcal{S}}, y} \sum_{i \in \mathcal{S}} \frac{1}{2} \begin{bmatrix} x_i \\ y \end{bmatrix}^\top \begin{bmatrix} H_i^{xx} & H_i^{xy} \\ H_i^{xy\top} & H_i^{yy} \end{bmatrix} \begin{bmatrix} x_i \\ y \end{bmatrix} + \begin{bmatrix} h_i^x \\ h_i^y \end{bmatrix}^\top \begin{bmatrix} x_i \\ y \end{bmatrix} \quad (1a)$$

$$\text{subject to } \begin{bmatrix} A_i^x & A_i^y \end{bmatrix} \begin{bmatrix} x_i^\top & y^\top \end{bmatrix}^\top - b_i = 0, \quad i \in \mathcal{S}, \quad (1b)$$

$$\begin{bmatrix} B_i^x & B_i^y \end{bmatrix} \begin{bmatrix} x_i^\top & y^\top \end{bmatrix}^\top - d_i \leq 0, \quad i \in \mathcal{S}, \quad (1c)$$

$$A^y y - b^y = 0, \quad B^y y - d^y \leq 0. \quad (1d)$$

Here, the global decision vector $x = [x_1, \dots, x_S]^\top$ is composed of local decision variables $x_i \in \mathbb{R}^{n_{xi}}$, where each x_i belongs to one subsystem $i \in \mathcal{S}$. The decision variables $y \in \mathbb{R}^{n_y}$ are “global” in the sense that they belong to the interconnecting infrastructure network, described by the constraints (1d). Each coefficient matrix/vector in the objective (1a) and the constraints (1b), (1c) belongs to one $i \in \mathcal{S}$.

Observe that problem (1) is defined over a star graph, where y and constraint (1d) correspond to the root vertex, and x_i and constraints (1b), (1c) belong/couple the root vertex to all leaves (Figure 1). This structure is common in many infrastructure networks such as electricity grids, gas networks or district heating systems, which are composed

of a network as the root and complex subsystems such as households, distribution grids or industrial facilities as leafs [7–12]. These applications often require a high degree of feasibility in a small number of iterations without full model exchange. The main objective of this work is to develop primal decomposition schemes able to achieve that goal.

3. Primal Decomposition Schemes

In contrast to duality-based techniques such as ADMM or dual decomposition, primal decomposition decomposes entirely in the primal space, i.e. no dual variables are updated in the solution process. The main idea here is to replace the subproblems in (1) by their optimal value functions. Specifically, one reformulates (1) as

$$\min_y \sum_{i \in \mathcal{S}} \phi_i(y), \quad \text{s.t.} \quad A^y y - b^y = 0, \quad B^y y - d^y \leq 0, \quad (2)$$

where for all $i \in \mathcal{S}$, the value function ϕ_i is defined as

$$\phi_i(y) \doteq \min_{x_i} \frac{1}{2} \begin{bmatrix} x_i \\ y \end{bmatrix}^\top \begin{bmatrix} H_i^{xx} & H_i^{xy} \\ H_i^{xy\top} & H_i^{yy} \end{bmatrix} \begin{bmatrix} x_i \\ y \end{bmatrix} + \begin{bmatrix} h_i^x \\ h_i^y \end{bmatrix}^\top \begin{bmatrix} x_i \\ y \end{bmatrix} \quad (3a)$$

$$\text{subject to} \quad \begin{bmatrix} A_i^x & A_i^y \end{bmatrix} \begin{bmatrix} x_i^\top & y^\top \end{bmatrix}^\top - b_i = 0, \quad i \in \mathcal{S}, \quad (3b)$$

$$\begin{bmatrix} B_i^x & B_i^y \end{bmatrix} \begin{bmatrix} x_i^\top & y^\top \end{bmatrix}^\top - d_i \leq 0, \quad i \in \mathcal{S}. \quad (3c)$$

The key idea is to apply standard algorithms for solving (2) by optimizing only with respect to the coupling variables y . Doing so can lead to enhanced robustness, as the complexity of the subproblems is not exposed to the algorithm solving (2).

Algorithms for solving (2) typically require first-order and possibly second-order derivatives of all $\{\phi_i\}_{i \in \mathcal{S}}$. Since all $\{\phi_i\}_{i \in \mathcal{S}}$ are non-smooth because of the inequality constraints, one typically relies on smooth reformulations. Inspired by interior-point methods [22], we introduce log-barrier functions and slack variables $s_i \in \mathbb{R}^{n_{ii}}$, which approximate (3) by

$$\Phi_i^\delta(y) \doteq \min_{x_i, s_i} \frac{1}{2} \begin{bmatrix} x_i \\ y \end{bmatrix}^\top \begin{bmatrix} H_i^{xx} & H_i^{xy} \\ H_i^{xy\top} & H_i^{yy} \end{bmatrix} \begin{bmatrix} x_i \\ y \end{bmatrix} + \begin{bmatrix} h_i^x \\ h_i^y \end{bmatrix}^\top \begin{bmatrix} x_i \\ y \end{bmatrix} - \delta \mathbf{1}^\top \ln(s_i) \quad (4a)$$

$$\text{subject to} \quad \begin{bmatrix} A_i^x & A_i^y \end{bmatrix} \begin{bmatrix} x_i^\top & y^\top \end{bmatrix}^\top - b_i = 0, \quad i \in \mathcal{S}, \quad (4b)$$

$$\begin{bmatrix} B_i^x & B_i^y \end{bmatrix} \begin{bmatrix} x_i^\top & y^\top \end{bmatrix}^\top - d_i + s_i = 0, \quad i \in \mathcal{S}, \quad (4c)$$

where $\delta \in \mathbb{R}_+$ is a barrier parameter, $\mathbf{1} \doteq [1, \dots, 1]^\top$, and the $\ln(\cdot)$ is evaluated component-wise. Note that $\lim_{\delta \rightarrow 0} \Phi_i^\delta(y) = \phi_i(y)$, and that Φ_i^δ is smooth¹. A basic primal decomposition strategy with smoothing is summarized in Algorithm 1.

¹Under standard regularity assumptions [23, A1-C1].

Algorithm 1: A basic primal decomposition scheme.

Initialize y^0, δ^0 .

while not terminated **do**

- 1) Solve (2) for $\phi_i \equiv \Phi_i^\delta$ with a NLP solver; in case the NLP solver calls $(\nabla_y \Phi_i^\delta, \nabla_y^2 \Phi_i^\delta)$, compute them locally for all $i \in \mathcal{S}$.
- 2) Decrease δ .

end

Return $y^k, \{x_i^k\}_{i \in \mathcal{S}}$.

Dealing With Infeasibility

An issue in Algorithm 1 is that the subproblems (3) may be infeasible for a given y . One way of circumventing this is to introduce auxiliary variables $z_i \in \mathbb{R}^{n_y}$ and to use relaxation techniques either based on augmented Lagrangians or on exact ℓ_1 -penalties. Consider a set of auxiliary variables $\{z_i\}_{i \in \mathcal{S}}$ and introduce additional constraints $z_i = y$ for all $i \in \mathcal{S}$. Then, we reformulate (4) equivalently ²

$$\Phi_i^\delta(y) = \min_{x_i, s_i, z_i} \frac{1}{2} \begin{bmatrix} x_i \\ y \end{bmatrix}^\top \begin{bmatrix} H_i^{xx} & H_i^{xy} \\ H_i^{xy^\top} & H_i^{yy} \end{bmatrix} \begin{bmatrix} x_i \\ y \end{bmatrix} + \begin{bmatrix} h_i^x \\ h_i^y \end{bmatrix}^\top \begin{bmatrix} x_i \\ y \end{bmatrix} - \delta \mathbf{1}^\top \ln(s_i) \quad (5a)$$

$$\text{subject to } \begin{bmatrix} A_i^x & A_i^y \end{bmatrix} \begin{bmatrix} x_i^\top & z_i^\top \end{bmatrix}^\top - b_i = 0, \quad i \in \mathcal{S}, \quad (5b)$$

$$\begin{bmatrix} B_i^x & B_i^y \end{bmatrix} \begin{bmatrix} x_i^\top & z_i^\top \end{bmatrix}^\top - d_i + s_i = 0, \quad i \in \mathcal{S}, \quad (5c)$$

$$z_i = y, \quad i \in \mathcal{S}, \quad (5d)$$

which can still be infeasible, but paves the way for augmented Lagrangian and exact ℓ_1 relaxations.

Augmented Lagrangian Relaxation

A simple way of making (5) feasible for all y is to relax (5d) via a quadratic penalty [22]. However, in this case, large penalty parameters might lead to numerical difficulties and feasibility can in general not be guaranteed for a finite penalty parameter. Hence, we use an Augmented Lagrangian (AL) approach to solve (2) for late outer iterations with a constant barrier parameter δ . Assigning the Lagrange multiplier λ_i to (5d), we relax (5d) in an Augmented Lagrangian fashion by adding the terms $\lambda_i^{k\top}(y - z_i) + \frac{\rho}{2}\|y - z_i\|_2^2$ to

²Observe that we have replaced y by z_i in the constraints here but not in the objective. Exchanging y in the objective is possible but might lead to a different numerical behavior.

Algorithm 2: AL-based primal decomposition.

Initialize $y^0, \delta^0, \rho^0; \lambda_i = 0, i \in \mathcal{S}$.

while phase 1 **do**

- 1) Solve the master problem (2) for $\phi_i \equiv \Phi_i^{\delta, \rho}$ with a NLP solver; in case the NLP solver calls $\phi_i(y^k), \nabla_y \phi_i(y^k)$, or $\nabla_{yy}^2 \phi_i(y^k)$, broadcast y^k to all $i \in \mathcal{S}$ and compute them locally.
- 2) Decrease δ , increase ρ .

end

while phase 2 **do**

- 3) Solve (2) as in phase 1.
- 4) Broadcast y^k to all $i \in \mathcal{S}$ and update λ_i^k by (7).

end

Return $y^k, \{x_i^k\}_{i \in \mathcal{S}}$.

Algorithm 3: ℓ_1 -based primal decomposition.

Initialize $y^0, \delta^0, \bar{\lambda}$ large enough.

while not terminated **do**

- 1) Solve the master problem (2) for $\phi_i \equiv \Phi_i^{\delta, \bar{\lambda}}$ with a NLP solver; in case the NLP solver calls $\phi_i(y^k), \nabla_y \phi_i(y^k)$, or $\nabla_{yy}^2 \phi_i(y^k)$, broadcast y^k to all $i \in \mathcal{S}$ and compute them locally.
- 2) Decrease δ .

end

Return $y^k, \{x_i^k\}_{i \in \mathcal{S}}$.

the objective:

$$\begin{aligned}
\Phi_i^{\delta, \rho}(y, \lambda_i^k) \doteq \min_{x_i, s_i, z_i} \frac{1}{2} \begin{bmatrix} x_i \\ y \\ z_i \end{bmatrix}^\top \begin{bmatrix} H_i^{xx} & H_i^{xy} & 0 \\ H_i^{xy\top} & H_i^{yy} + \rho I & -\rho I \\ 0 & -\rho I & \rho I \end{bmatrix} \begin{bmatrix} x_i \\ y \\ z_i \end{bmatrix} + \begin{bmatrix} h_i^x \\ h_i^y + \lambda_i^k \\ -\lambda_i^k \end{bmatrix}^\top \begin{bmatrix} x_i \\ y \\ z_i \end{bmatrix} - \delta \mathbf{1}^\top \ln(s_i) \\
\text{s.t.} \quad [A_i^x \quad A_i^y] \begin{bmatrix} x_i^\top & z_i^\top \end{bmatrix}^\top - b_i = 0, \mid \gamma_i \\
[B_i^x \quad B_i^y] \begin{bmatrix} x_i^\top & z_i^\top \end{bmatrix}^\top + s_i - d_i = 0, \mid \mu_i.
\end{aligned} \tag{6}$$

Here, (γ_i, μ_i) are Lagrange multipliers corresponding to the constraints in the same line. Note that the solution of (6) can be forced to be arbitrarily close to that of (5) by letting $\rho \rightarrow \infty$, if (6) is feasible for y . In addition, if one has a good Lagrange multiplier estimate $\lambda^k \approx \lambda^*$, (5) and (6) are equivalent for a finite $\rho < \infty$ [29, Sec. 3.2.1], [30, Thm. 17.5]. We will exploit this fact in the following.

Primal decomposition based on the augmented Lagrangian works as follows: In phase 1, the barrier parameter δ and the penalty parameter ρ are increased/decreased simultaneously. In phase 2, when δ/ρ are sufficiently small/large, both are held constant and a standard augmented Lagrangian algorithm is applied to the resulting optimization

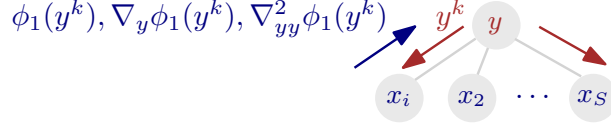


Figure 2: Communication in Algorithms 2 and 3.

problem to obtain feasibility in (5d). We use the standard first-order update rule from augmented Lagrangian algorithms [30, Chap. 17.3]

$$\lambda_i^{k+1} = \lambda_i^k + \rho(y^k - z_i^k). \quad (7)$$

The resulting scheme is summarized in Algorithm 2.

ℓ_1 -penalty relaxation

A second variant to ensure feasibility is to relax (5d) via an ℓ_1 -penalty function. This has the advantage that it is exact also for a finite penalty parameter $\bar{\lambda} \in \mathbb{R}_+$ without the need for Lagrange-multiplier estimation. By doing so, the objective becomes non-smooth. However, the non-smoothness can be eliminated by using an elastic relaxation [30, p.535]: the ℓ_1 -penalty $\min_{y,z_i} \|y - z_i\|_1$ is reformulated by introducing two non-negative auxiliary variables $v_i, w_i \in \mathbb{R}_+^{n_y}$ as $\min_{y,z_i,v_i,w_i} v_i + w_i$ subject to $y - z_i = v_i - w_i$. The corresponding reformulation of (5) reads

$$\begin{aligned} \Phi_i^{\delta,\bar{\lambda}}(y) \doteq & \min_{\substack{x_i, s_i, z_i \\ v_i, w_i}} \frac{1}{2} \begin{bmatrix} x_i \\ z_i \end{bmatrix}^\top \begin{bmatrix} H_i^{xx} & H_i^{xy} \\ H_i^{xy^\top} & H_i^{yy} \end{bmatrix} \begin{bmatrix} x_i \\ z_i \end{bmatrix} + \begin{bmatrix} h_i^x \\ h_i^y \end{bmatrix}^\top \begin{bmatrix} x_i \\ z_i \end{bmatrix} \\ & + \bar{\lambda} \mathbf{1}^\top (v_i + w_i) - \delta (\mathbf{1}^\top \ln(s_i) + \mathbf{1}^\top \ln(v_i) + \mathbf{1}^\top \ln(w_i)) \quad (8) \\ \text{s.t. } & \begin{bmatrix} A_i^x & A_i^y \end{bmatrix} \begin{bmatrix} x_i^\top & z_i^\top \end{bmatrix}^\top - b_i = 0, \quad | \gamma_i, \\ & \begin{bmatrix} B_i^x & B_i^y \end{bmatrix} \begin{bmatrix} x_i^\top & z_i^\top \end{bmatrix}^\top + s_i - d_i = 0, \quad | \mu_i, \\ & y - z_i - v_i + w_i = 0, \quad | \chi_i, \end{aligned}$$

where the bounds $(v_i, w_i) \geq 0$ are replaced by log-barrier functions. If one chooses $\bar{\lambda} < \infty$ large enough, (5) and (8) are equivalent [30, Thm 17.3].

Primal decomposition based on the ℓ_1 -penalty solves (2) using $\Phi_i^{\delta,\bar{\lambda}}$ with a fixed $\bar{\lambda}$ larger than a certain threshold and decreases the barrier parameter δ during the iterations. The overall algorithm is summarized in Algorithm 3.

The communication of Algorithm 1 and 2 is illustrated in Figure 2. Communication involves $\phi_i(y)$, its derivatives, and λ_i . Hence, the dimension of information exchange depends only on the dimension of coupling variables n_y .

4. Computing sensitivities

Next, we review how to compute $\nabla_y \Phi_i^\delta$ and $\nabla_{yy}^2 \Phi_i^\delta$ under standard regularity assumptions based on the implicit function theorem [23]. Reformulate (4) by

$$\begin{aligned} \Phi_i^\delta(y) &= \min_{x_i, s_i} f_i^\delta(x_i, s_i; y) \\ \text{subject to} \quad & g_i(x_i; y) = 0 \mid \gamma_i, \quad h_i(x_i; y) + s_i = 0 \mid \mu_i, \end{aligned} \quad (9)$$

where f_i^δ is defined by (4a), and g_i and h_i are defined by (4b), (4c). Define the Lagrangian to (9),

$$L_i^\delta(x_i, s_i, \gamma_i, \mu_i; y) \doteq f_i^\delta(x_i, s_i; y) + \gamma_i^\top g_i(x_i; y) + \mu_i^\top (h_i(x_i; y) + s_i).$$

Assume that (9) is feasible for a given y and that the regularity conditions from [23, Ass. 1-4] hold. Then, the KKT conditions to (9) form an implicit function in form of $F_i^\delta(x_i^*, s_i^*, \gamma_i^*, \mu_i^*; y) = 0$, where the superscript $(\cdot)^*$ indicates a KKT stationary point. Thus, by the implicit function theorem, there exist a neighborhood around y for which there exists functions $p_i^*(y) \doteq (x_i^*(y), s_i^*(y), \gamma_i^*(y), \mu_i^*(y))$ such that $F_i^\delta(p_i^*(y); y) = 0$. Hence, we can rewrite (9) as $\Phi_i^\delta(y) = f_i^\delta(x_i^*(y), s_i^*(y); y) = L_i(p_i^*(y); y)$ since $p_i^*(y)$ is feasible.

Applying the total derivative and the chain rule yields

$$\nabla_y \Phi_i^\delta(y) = \nabla_y L_i^\delta(p_i^*(y); y) + \nabla_{p_i^*} L_i^\delta(p_i^*(y); y) \nabla_y p_i^*(y).$$

By the KKT conditions, we have that $\nabla_{p_i^*} L_i^\delta(p_i^*(y); y) = 0$ and thus

$$\nabla_y \Phi_i^\delta(y) = \nabla_y L_i^\delta(p_i^*(y); y). \quad (10)$$

Again by the total derivative, the Hessian can be computed by

$$\nabla_{yy}^2 \Phi_i^\delta(y) = \nabla_{yy}^2 L_i(p_i^*(y); y) + \nabla_{yp_i^*}^2 L_i(p_i^*(y); y) \nabla_y p_i^*(y). \quad (11)$$

It remains to derive an expression for $\nabla_y p_i^*(y)$. The KKT conditions of (9) read

$$F_i^\delta(x_i^*, s_i^*, \gamma_i^*, \mu_i^*; y) = \begin{bmatrix} \nabla_{x_i} f_i(x_i^*, y) + \nabla_{x_i} g_i(x_i^*, y) \gamma_i^* + \nabla_{x_i} h_i(x_i^*, y) \mu_i^* \\ -\delta S_i^{*-1} \mathbf{1} + \mu_i^* \\ g_i(x_i^*, y) \\ h_i(x_i^*, y) + s_i^* \end{bmatrix} \stackrel{!}{=} 0,$$

where $S_i^* = \text{diag}(s_i^*)$. By the total differential and the chain rule we have $\nabla_y F_i^\delta(p_i^*(y), y) + \nabla_{p_i^*} F_i^\delta(p_i^*(y), y) \nabla_y p_i^*(y) = 0$. Hence, we can compute the Jacobian $\nabla_y p_i^*(y)$ by solving the system of linear equations

$$\left(\nabla_{p_i^*} F_i^\delta(p_i^*(y), y) \right) \nabla_y p_i^*(y) = -\nabla_y F_i^\delta(p_i^*(y), y). \quad (12)$$

Observe that (12) is a system of linear equations with multiple right-hand sides. In summary, we can compute $\nabla_{yy}^2 \Phi_i^\delta(y)$ locally for each $i \in \mathcal{S}$ by combining (11) and (12). The corresponding formulas for the gradient and the Hessian of $\Phi_i^{\delta, \rho}$ and $\Phi_i^{\delta, \bar{\lambda}}$ from (6) and (8), i.e. of the AL relaxation and the ℓ_1 relaxation (9) are given in Appendix A.

5. A Method for Solving the Master Problem

An important question is how to solve the master problem (2) for different variants of ϕ_i . In general, this can be done by any sensitivity-based NLP solver. We proceed by showing how to obtain a simple globalized version of Algorithm 1 based on a line-search scheme; here, the idea is to show global convergence for the relaxed problem (2) with $\phi_i \in \{\Phi_i^{\delta,\rho}, \Phi_i^{\delta,\bar{\lambda}}\}$ for fixed penalty and barrier parameters. This leads to converge of a solution to the original problem (1) by standard results from penalty and barrier methods [30, Thms. 17.1, 17.6].

Define the objective of (2), $\psi(y) \doteq \sum_{i \in \mathcal{S}} \phi_i(y)$, as a global merit function, where $\phi_i \in \{\Phi_i^{\delta,\rho}, \Phi_i^{\delta,\bar{\lambda}}\}$. The basic idea is to employ a Sequential Quadratic Programming (SQP) scheme, where we ensure a sufficient decrease in ψ at each step via the Armijo condition. The overall algorithm is summarized in Algorithm 4. Similar to the general primal decomposition scheme from Algorithm 1, the master problem solver evaluates the sensitivities $(\nabla_y \phi_i, \nabla_{yy}^2 \phi_i)$ in step (i), in order to construct a quadratic approximation of (2) in step (ii). Solving this approximation yields a search direction Δy . The stepsize α is updated with a backtracking line-search with the Armijo condition as termination criterion.

Global Convergence

We now establish global convergence³ of Algorithm 4 to a minimizer of the relaxed problems (2) for $\phi_i \in \{\Phi_i^{\delta,\rho}, \Phi_i^{\delta,\bar{\lambda}}\}$. Assume that the following regularity assumptions hold at the optimal solution at $p^* \doteq [p_i^*(y^*)]_{i \in \mathcal{S}}$.

Assumption 1 (Subproblem regularity). *Assume that $\forall i \in \mathcal{S}$:*

- a) $\begin{bmatrix} \Delta x_i^* \\ \Delta y^* \end{bmatrix}^\top \begin{bmatrix} H_i^{xx} & H_i^{xy} \\ H_i^{xy\top} & H_i^{yy} \end{bmatrix} \begin{bmatrix} \Delta x_i^* \\ \Delta y^* \end{bmatrix} > 0$, for all $\begin{bmatrix} \Delta x_i^* \\ \Delta y^* \end{bmatrix} \neq 0$ with $\begin{bmatrix} A_i^x & A_i^y \end{bmatrix} \begin{bmatrix} \Delta x_i^* \\ \Delta y^* \end{bmatrix} = 0$;
- b) $\begin{bmatrix} A_i^x & A_i^y \\ B_i^x & B_i^y \end{bmatrix}$ has full row rank;
- c) $[\mu_i^*]_j + [B_i^x \ B_i^y][x_i^{*\top} \ y^{*\top}]^\top]_j \neq 0$, $\forall j = 1, \dots, \text{nr}(B_i^x)$.

Assumption 2 (Master problem regularity). *Assume that $\begin{bmatrix} A^y{}^\top & B^y{}^\top \end{bmatrix}^\top$ has full row rank.*

Line-search methods require that the search direction Δy is a descent direction, i.e. $\Delta y (\sum_{i \in \mathcal{S}} \nabla_i \phi_i(y)) < 0$. This can be ensured by showing that $\sum_{i \in \mathcal{S}} \nabla_{yy}^2 \phi_i \succ 0$ for all variants of ϕ_i , which we do with the next lemma.

³We use the definition of global convergence in the context of NLPs, i.e. the convergence to a KKT point from an arbitrary initialization [30, Chap. 3]. However, since problems (1) and (2) are strongly convex and we assume regularity in Assumption 1, every KKT point is also a global minimizer.

Algorithm 4: A simple master problem solver.

Initialize $y^0, \epsilon, \delta, \zeta \in (0, 1), \rho$ or $\bar{\lambda}, \phi_i \in \{\Phi_i^{\delta, \rho}, \Phi_i^{\delta, \bar{\lambda}}\}$.
while $\|\Delta y\| > 0$ **do**
 1) Evaluate $(\nabla_y \phi_i, \nabla_{yy}^2 \phi_i)$ locally for all $i \in \mathcal{S}$ for given (δ, ρ) or $(\delta, \bar{\lambda})$.
 2) Solve the coordination problem

$$\min_{\Delta y} \sum_{i \in \mathcal{S}} \frac{1}{2} \Delta y \nabla_{yy}^2 \phi_i(y) \Delta y^\top + \nabla_y \phi_i(y)^\top \Delta y \quad (13)$$
 s.t. $A^y(y + \Delta y) - b^y = 0, B^y(y + \Delta y) - b^y \leq 0$.
 3) Line search: $\alpha = 1$;
 while $\psi(y) - \psi(y + \alpha \Delta y) \geq -\sigma \alpha \nabla_y \psi(y)^\top \Delta y$ **do**
 | $\alpha \leftarrow \zeta \alpha$
 end
 4) Update $y \leftarrow y + \alpha \Delta y$.
 5) Decrease δ , increase $(\rho, \bar{\delta})$.
end
Return $y, \{x_i\}_{i \in \mathcal{S}}$.

Lemma 1 (Positive definite Hessians). *Let Assumption 1 hold and assume that $(s_i, \mu_i, v_i, w_i) > 0$. Then, a), the Hessian $\nabla_{yy}^2 \Phi_i^{\delta, \rho}$ is positive definite for all $\rho > 0$. Moreover, b), $\nabla_{yy}^2 \Phi_i^{\delta, \bar{\lambda}}$ is positive definite if $\bar{\lambda}$ is larger than all multipliers associated to the elastic constraints $\bar{\lambda} > \max_j |\chi_j^*|$.*

The proof of Lemma 1 is given in Appendix B. Now we are able to show global convergence of Algorithm 4 to the solution of problem (2) with $\phi_i \in \{\Phi_i^{\delta, \rho}, \Phi_i^{\delta, \bar{\lambda}}\}$ for fixed penalty and barrier parameters.

Theorem 1 (Convergence of Algorithm 4 for fixed $\delta, \rho, \bar{\lambda}$). *Consider Algorithm 4 with either fixed (δ, ρ, λ) if $\phi_i = \Phi_i^{\delta, \rho}$ or with fixed $(\delta, \bar{\lambda})$ if $\phi_i = \Phi_i^{\delta, \bar{\lambda}}$. Let Assumptions 1, 2 and the conditions of Lemma 1 hold. Then, the iterates generated by Algorithm 4 converge to the global minimizer of problem (2) with $\phi_i \in \{\Phi_i^{\delta, \rho}, \Phi_i^{\delta, \bar{\lambda}}\}$.*

Proof. The unconstrained minimizer to (13), $\Delta y = -\sum_{i \in \mathcal{S}} \nabla_{yy}^2 \phi_i^{-1}(y) \sum_{i \in \mathcal{S}} \nabla_y \phi_i(y)$, is a descent direction for the merit function $\psi(\cdot)$ since $\sum_{i \in \mathcal{S}} \nabla_y \phi_i(y)^\top \Delta y < 0$ by the positive definiteness of the Hessians from Lemma 1. Observe that $\Delta y = 0$ is feasible for (13) by feasibility of y . This shows that either $\Delta y = 0$, or Δy is a descent direction. Hence, by [30, Lem 3.1], there exists an $\alpha \in (0, 1]$ such that $\psi(y) - \psi(y + \alpha \Delta y) \geq -\sigma \alpha \nabla_y \psi(y)^\top \Delta y$ is satisfied and thus the inner while loop is well defined. Moreover, by the convergence of line-search methods [29, Prop 1.2.1], Algorithm 4 will either converge to a stationary point of ψ returning $\Delta y = 0$, or, alternatively, if the unconstrained search direction is blocked by the constraints in (13), $\Delta y = 0$ is returned since $\Delta y = 0$ is feasible.

We now show that y is optimal for (2) if $\Delta y = 0$. The KKT conditions associated to (13) read

$$\begin{cases} \sum_{i \in \mathcal{S}} \nabla_{yy}^2 \phi_i(y) \Delta y + \nabla_y \phi_i(y)^\top + A^y{}^\top \gamma_y + B^y{}^\top \mu_y = 0 \\ A^y(y + \Delta y) - b^y = 0, \quad B^y(y + \Delta y) - b^y \leq 0, \\ (B^y(y + \Delta y) - b^y)^\top \mu = 0, \quad \mu \geq 0, \end{cases}$$

which are precisely the KKT conditions for (2) if $\Delta y = 0$. Since (2) is convex, and Assumptions 1 and 2 hold, the assertion follows. \square

Combining Theorem 1 with the convergence results for the ℓ_1 -penalty method [30, Thm 17.3] or the augmented Lagrangian method [31, Prop 2.7] implies convergence of Algorithm 4 to the minimizer of the original problem (1) for sufficiently large penalties.

Remark 1 (Satisfying the assumptions of Theorem 1). *Observe that the assumptions for Theorem 1 are standard regularity assumptions from nonlinear programming [23, Ass. 1-4]. Moreover, $(s_i, \mu_i, v_i, w_i) > 0$ is always ensured when using interior-point solvers for solving (5) and (6) even in the case of early termination.*

Remark 2 (Convergence rate). *Since phase 1 of Algorithm 2 is a combination of a quadratic penalty and an interior point method, one can achieve up to a superlinear local convergence rate when decreasing/increasing δ/ρ fast enough since the only limiting factor is the Newton step [30, Chap 17.1, Chap 19.8]. A too fast increase/decrease, however, leads to numerical difficulties in Newton step computations. In phase 2, the algorithm switches to a augmented Lagrangian method, where one can expect linear convergence to the barrier problem (4), cf. [31, Prop 2.7].*

6. Implementation Aspects

The evaluation of the sensitivities of $\phi_i \in \{\Phi_i^{\delta, \rho}, \Phi_i^{\delta, \bar{\lambda}}\}$ requires solving local optimization problems (6) or (8) for fixed $\delta, \rho, \bar{\lambda}$. This can be done using specialized and optimized interior-point solvers, if they allow termination once a certain barrier δ is reached. Moreover, interior-point solvers factorize the KKT matrices $\nabla_{p_i} F_i^\delta$ (cf. (24), (26)) at each inner iteration and these factorizations can be re-used for Hessian computation via (12). Here we provide two variants: our own interior-point QP solver based on standard techniques for stepsize selection and barrier parameter decrease [30, Chap. 16.6] and the option to use third-party solvers such as Ipopt [32].

In early iterations, it is typically not necessary to solve the local problems to a high precision, since the barrier parameter δ is still large and the penalty parameters $(\rho, \bar{\lambda})$ are still small. Hence, we solve the subproblems to an accuracy measured in the violation of the optimality conditions $\|F_i^\delta(p_i^k, y^k)\|_\infty$ and terminate if $\|F_i^\delta(p_i^k, y^k)\|_\infty < \min(\delta, 1/\rho)$ or $\|F_i^\delta(p_i^k, y^k)\|_\infty < \min(\delta, 1/\bar{\lambda})$. This is inspired by the termination of inexact interior-point methods [33]. Warm-starting the local solves with the solution of the previous iteration reduces computation time significantly.

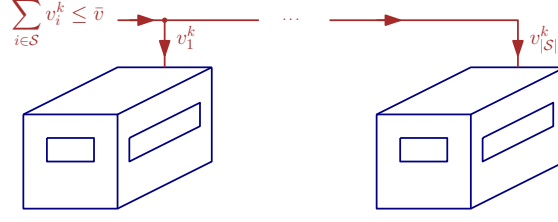


Figure 3: Buildings connected via network with limited capacity.

Numerical Linear Algebra

Efficient numerical linear algebra is crucial for performance. The most expensive steps in terms of memory and CPU time are the factorization of the local KKT matrices and the backsolves in (12). Since we only consider QPs, large parts of the KKT matrices in (12) are constant over the iterations, which can be exploited for pre-computation. Here, we make heavy use of the Schur complement. Details on how to achieve this for the AL formulation are given in Appendix A.

Updating Penalties

We use simple update rules for the penalty parameters. They are

$$\delta^{k+1} = 0.2\delta^k, \quad \bar{\lambda}^{k+1} = 2\bar{\lambda}^k, \quad \rho^{k+1} = 3\rho^k,$$

with initial values $\delta^0 = 0.1$, $\rho^0 = 10^3$, and $\bar{\lambda}^0 = 100$. After a fixed amount of 8 iterations, phase 2 starts and the above values stay constant. The parameters in the update rules are found via tuning in typical ranges for interior point methods, augmented Lagrangian and ℓ_1 -penalty methods [30, Chapters 17.1, 17.2, Eq. 19.18]. They terminate with $(\delta^\infty, \bar{\lambda}^\infty, \rho^\infty) = (10^{-8}, 2.6 \cdot 10^4, 6.6 \cdot 10^6)$. Moreover, IPOPT terminates with penalty $\delta^\infty = 10^{-8} \dots 10^{-9}$ for the examples considered.⁴

7. Numerical Case Studies

We consider an optimal control problem for a city district with a scalable number of commercial buildings connected via a electricity grid with limited capacity. The building data is from [34]. We neglect the waterside HVAC system and assume that the buildings are equipped with heat pumps with a constant coefficient of performance.

7.1. District HVAC

The evolution of the temperature of the m th zone in the i th building reads

$$C_{m,i}(T_{m,i}^{k+1} - T_{m,i}^k) = -H_{m,i}(T_{m,i}^k - T_a^k) - \sum_{n \in \mathcal{Z}_i} G_{mn,i}(T_{m,i}^k - T_{n,i}^k) - \dot{Q}_{m,i}^{ck} + \dot{Q}_{m,i}^{dk}, \quad (14)$$

⁴Note that IPOPT uses μ as symbol for the penatly parameter.

where at time step k , $T_{m,i}^k$ is the temperature of zone m and T_a^k the ambient temperature, $C_{i,m}$ is the thermal capacity, $H_{m,i}$ and $G_{mn,i}$ are heat transfer coefficients with the ambient and between two zones. Moreover, $(\dot{Q}_{m,i}^{ck}, \dot{Q}_{m,i}^{dk})$ are the controllable/uncontrollable heat influxes from the heat pump and from sources of disturbance such as solar irradiation and occupancy. Eq. (14) can be written in compact form as

$$C_i(T_i^{k+1} - T_i^k) = -H_i(T_i^k - T_a^k) - G_i T_i^k - \dot{Q}_i^{ck} + \dot{Q}_i^{dk},$$

where $T_i^\top \doteq [T_{1,i}, \dots, T_{|Z_i|,i}]$, $\dot{Q}_i^{ck^\top} \doteq [\dot{Q}_{1,i}^{ck}, \dots, \dot{Q}_{n_z,i}^{ck}]$ and $\dot{Q}_i^{dk^\top} \doteq [\dot{Q}_{1,i}^{dk}, \dots, \dot{Q}_{n_z,i}^{dk}]$. This yields a state-space model

$$\begin{aligned} T_i^{k+1} &\doteq z_i^{k+1} = (I - C_i^{-1}(H_i + G_i)) T_i^k - C_i^{-1} \dot{Q}_i^{ck} + C_i^{-1} [H_i \quad I] [T_a^{k^\top} \quad \dot{Q}_i^{dk^\top}]^\top \\ &\doteq A_i x^k + B_i u_i^k + E_i d_i^k. \end{aligned} \quad (15)$$

Stacking the above over N time steps yields

$$\begin{aligned} \bar{z}_i &= \begin{bmatrix} 0 & 0 \\ I_{N-1} \otimes A_i & 0 \end{bmatrix} \bar{z}_i + \begin{bmatrix} 0 \\ I_{N-1} \otimes B_i \end{bmatrix} \bar{u}_i + \begin{bmatrix} 0 \\ I_{N-1} \otimes E_i \end{bmatrix} \bar{d}_i + \bar{z}_i^f \\ &\doteq \bar{A}_i \bar{z}_i + \bar{B}_i \bar{u}_i + \bar{E}_i \bar{d}_i + \bar{z}_i^f, \end{aligned}$$

where $\bar{z}_i^\top \doteq [z_i^{0^\top}, \dots, z_i^{N^\top}]$, $\bar{u}_i^\top \doteq [u_i^{1^\top}, \dots, u_i^{N^\top}]$, $\bar{d}_i^\top \doteq [d_i^{1^\top}, \dots, d_i^{N^\top}]$, $\bar{z}_i^{f^\top} \doteq [z_i^f, 0^\top, \dots, 0^\top]$ and z_i^f are the initial temperatures. Define the total energy consumption of building $i \in \mathcal{S}$ at time step k by $v_i^k = \mathbf{1}^\top u_i^k$, and $\bar{v}_i^\top \doteq [v_i^{0^\top}, \dots, v_i^{N^\top}]$. Then, the above is equivalent to

$$[(I - \bar{A}_i) \quad -\bar{B}_i \quad 0] [\bar{z}_i^\top \quad \bar{u}_i^\top \quad \bar{v}_i^\top]^\top = \bar{E}_i \bar{d}_i + \bar{z}_i^f. \quad (16)$$

The grid coupling between all subsystems $i \in \mathcal{S}$ induces an upper-bounded energy supply writing as a global constraint: $\mathbf{1}^\top v_i^k \leq \bar{v}$ for all times k . Moreover, we have local comfort constraints $\underline{T} \mathbf{1} \leq z_i^k \leq \bar{T} \mathbf{1}$.

Optimal Control Problem

Assume that the goal of each building is to minimize its cost of energy consumption over N time steps respecting all constraints. The cost function to buy the power from the utility is given by $f_i^k(u_i^k) \doteq 0.5 c^k (u_i^k)^2 + g^k u_i^k$, where g^k is a linear and $c^k > 0$ is a (small) quadratic cost coefficient. This yields a discrete-time Optimal Control Problem (OCP) for building i ,

$$\begin{aligned} \phi_i(v_i) &\doteq \min_{\bar{z}_i, \bar{u}_i, \bar{v}_i} \frac{1}{2} \begin{bmatrix} \bar{z}_i^\top \\ \bar{u}_i^\top \\ \bar{v}_i^\top \end{bmatrix} \begin{bmatrix} 0 & 0 & 0 \\ 0 & cI & 0 \\ 0 & 0 & 0 \end{bmatrix} \begin{bmatrix} \bar{x}_i \\ \bar{u}_i \\ \bar{v}_i \end{bmatrix} + \begin{bmatrix} 0 \\ \mathbf{1}^\top \otimes g \end{bmatrix} \begin{bmatrix} \bar{z}_i \\ \bar{u}_i \\ \bar{v}_i \end{bmatrix} \\ \text{s.t. } (16), & \begin{bmatrix} I & 0 & 0 \\ -I & 0 & 0 \end{bmatrix} \begin{bmatrix} \bar{z}_i \\ \bar{u}_i \\ v_i \end{bmatrix} \leq \begin{bmatrix} \bar{T} \mathbf{1} \\ -\underline{T} \mathbf{1} \end{bmatrix}, \quad \bar{v}_i = I \otimes \mathbf{1}^\top \bar{u}_i. \end{aligned}$$

The overall OCP—including global grid constraints—reads

$$\min_{v_1, \dots, v_{|\mathcal{S}|}} \sum_{i \in \mathcal{S}} \phi_i(v_i), \text{ s.t. } (\mathbf{1}^\top \otimes I) [v_1^\top, \dots, v_{|\mathcal{S}|}^\top]^\top \leq \bar{v} \mathbf{1}. \quad (17)$$

To obtain a problem in form of (1), define $x_i^\top = [\bar{x}_i^\top, \bar{u}_i^\top, \bar{v}_i^\top]$, $i \in \mathcal{S}$, $y^\top = [v_1^\top, \dots, v_{|\mathcal{S}|}^\top]$, $H_i^x = \text{blkdiag}(0, cI, 0)$, $h_i^x = [0, \mathbf{1}^\top \otimes g, 0]^\top$, $h_i^y = 0$, $H_i^{xy} = 0$, $B_i^y = 0$, $d_i^\top = [\bar{T} \mathbf{1}^\top, -\bar{T} \mathbf{1}^\top]$,

$$A_i^x = \begin{bmatrix} (I - \bar{A}_i) & -\bar{B}_i & 0 \\ 0 & I \otimes \mathbf{1}^\top & 0 \end{bmatrix}, \quad A_i^y = \begin{bmatrix} 0 \\ -e_i^\top \otimes I \end{bmatrix}, \quad B_i^x = \begin{bmatrix} I & 0 & 0 \\ -I & 0 & 0 \end{bmatrix},$$

where e_i is the i th unit vector, $b_i^\top = [(\bar{E}_i \bar{d}_i + \bar{z}_i^f)^\top \quad 0]$, $A^y = 0$, $b^y = 0$, $B^y = \mathbf{1}^\top \otimes I$, and $d^y = \bar{v} \mathbf{1}$.

7.2. Optimal Power Flow

Optimal Power Flow (OPF) aims at minimizing the cost of power generation in power systems while satisfying all grid and generator constraints. A standard OPF formulation reads

$$\min_{g, \theta, f} \frac{1}{2} g^\top H g + g^\top h \quad (18a)$$

$$\text{subject to} \quad C^g g - d = -B\theta, \quad f = -B^b \theta, \quad (18b)$$

$$0 \leq g \leq \bar{g}, \quad -\bar{f} \leq f \leq \bar{f}, \quad (18c)$$

where $g \in \mathbb{R}^{n_g}$ is the active power generation of generators, the diagonal matrix H and vector h are composed of generator-specific cost coefficients, $d \in \mathbb{R}^{n_b}$ are active power demands and $\theta \in \mathbb{R}^{n_b}$ are voltage angles at each bus. In (18b), $B \in \mathbb{R}^{n_b \times n_b}$ is the bus susceptance matrix and $B^b \in \mathbb{R}^{n_b \times n_g}$ is the branch susceptance matrix, which map the voltage angles to power injections and power flows over transmission lines $f \in \mathbb{R}^{n_l}$ respectively, cf. [35]. The matrix $C^g \in \mathbb{R}^{n_b \times n_g}$ maps generator injections to connecting buses. The constraint (18c) expresses generation and line flow limits.

Power grids are typically structured in hierarchy levels reaching from extra-high voltage to low-voltage grids. As a numerical test case, we consider the **IEEE 300-bus** test system to which we connect a varying amount of **118-bus** sub-grids (with data from the MATPOWER database [36]). We add a small regularization term of 10^{-6} on the main diagonal of each H_{yy} to make the problem strongly convex in order to meet the conditions of Assumption 1.

To obtain a problem in form of (1), we introduce decision variables for the master grid $y = [g_0 \quad \theta_0 \quad f_0 \quad \bar{y}_0]$, where \bar{y}_0 is an auxiliary variable corresponding to the active power at interconnecting nodes with the lower-level network. For the i th lower-level subproblem

Table 1: Number of decision variables and constraints for the HVAC and OPF problems.

	$ \mathcal{S} $	n_x	n_y	n_e	n_i	n_{ey}	n_{iy}
HVAC	30	28,200	690	15,090	28,800	0	1,403
	180	169,200	4,140	90,540	172,800	0	8,303
	300	282,000	6,900	150,900	288,000	0	13,823
OPF	29	11,191	809	9,557	14,880	712	960
	64	23,756	844	20,232	31,680	712	960

we get

$$\begin{aligned}
\phi_i(y) &\doteq \min_{g_i, \theta_i, f_i} \frac{1}{2} \begin{bmatrix} g_i \\ \theta_i \\ f_i \\ y \end{bmatrix}^\top \begin{bmatrix} H_i & 0 \\ 0 & 0 \end{bmatrix} \begin{bmatrix} g_i \\ \theta_i \\ f_i \\ y \end{bmatrix} + \begin{bmatrix} h_i \\ 0 \end{bmatrix}^\top \begin{bmatrix} g_i \\ \theta_i \\ f_i \\ y \end{bmatrix} \\
\text{s.t. } &\begin{bmatrix} C_i^g & B_i & 0 & C_i^y \\ 0 & B_i^b & I & 0 \end{bmatrix} \begin{bmatrix} g_i & \theta_i & f_i & y \end{bmatrix}^\top = \begin{bmatrix} d_i \\ 0 \end{bmatrix}, \\
&\begin{bmatrix} I & 0 & 0 & 0 \\ -I & 0 & 0 & 0 \\ 0 & 0 & I & 0 \\ 0 & 0 & -I & 0 \end{bmatrix} \begin{bmatrix} g_i & \theta_i & f_i & y \end{bmatrix}^\top \leq \begin{bmatrix} \bar{g}_i \\ 0 \\ \bar{f}_i \\ \bar{f}_i \end{bmatrix}.
\end{aligned}$$

Here, C_i^y are a selection matrices, which couple power demand/generation at interconnecting nodes between subsystems. The master problem then reads

$$\begin{aligned}
\min_y \sum_{i \in \mathcal{S}} \phi_i(y) \quad &\text{subject to} \quad [\theta_0]_1 = 0, \\
&\begin{bmatrix} C_0^g & B_0 & 0 & C_0^y \\ 0 & B_0^b & I & 0 \end{bmatrix} \begin{bmatrix} g_0 & \theta_0 & f_0 & \bar{y}_0 \end{bmatrix}^\top = \begin{bmatrix} d_0 \\ 0 \end{bmatrix}, \\
&\begin{bmatrix} I & 0 & 0 & 0 \\ -I & 0 & 0 & 0 \\ 0 & 0 & I & 0 \\ 0 & 0 & -I & 0 \end{bmatrix} \begin{bmatrix} g_0 & \theta_0 & f_0 & \bar{y}_0 \end{bmatrix}^\top \leq \begin{bmatrix} \bar{g}_0 \\ 0 \\ \bar{f}_0 \\ \bar{f}_0 \end{bmatrix},
\end{aligned}$$

where $[\theta_0]_1 = 0$ is a reference (slack) constraint in order to obtain an unique angle solutions $\{\theta_i^*\}_{i \in \mathcal{S} \cup \{0\}}$, and C_0^y is a matrix mapping the coupling variables to coupling buses.

7.3. Numerical Results

We benchmark our algorithms against ADMM (as one of the most popular algorithms for decomposition) and against **Ipopt** v3.14.4 (as one of the most prominent centralized NLP solvers).⁵ The particular variant of ADMM can be found in an extended version of

⁵The ADMM-based QP solver **OSQP** solver did not converge for the problems presented here.

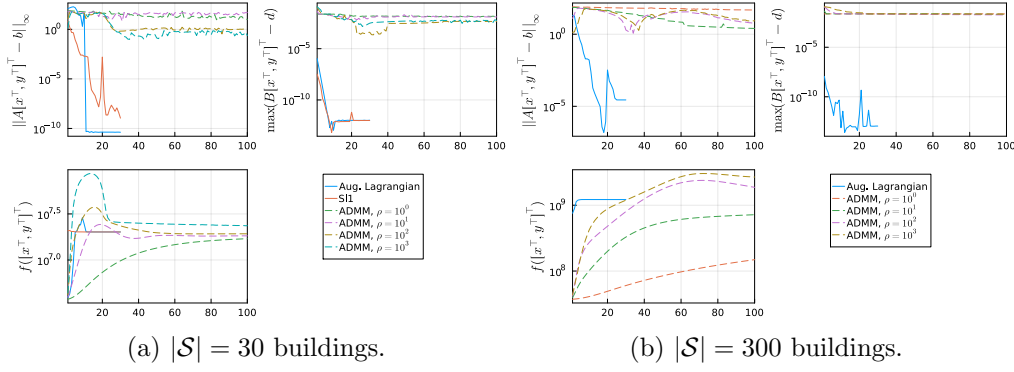


Figure 4: Convergence for three HVAC problems.

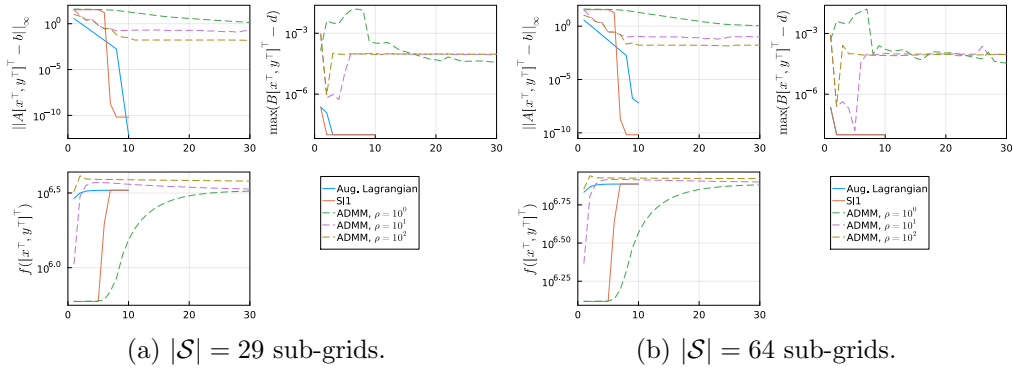


Figure 5: Convergence for two OPF problems.

this work [37]. We rely on **OSQP** v0.6.2 [38] for solving subproblems and the coordination problem in ADMM. In primal decomposition, we rely on our own interior-point solver for the subproblems and on Algorithm 4 for coordination, where we solve (13) via **Ipo**pt.⁶ We perform all simulations on a shared-memory virtual machine with 30 cores and 100GiB memory. The underlying hardware is exclusively used for the case studies. All algorithms are parallelized via Julia multi-threading—thus all subproblems are solved on multiple cores in parallel.

We compare the numerical performance of all algorithms on OCP (17) for $|\mathcal{S}| \in \{30, 180, 300\}$ buildings, and on the OPF problem (18) with $|\mathcal{S}| \in \{29, 64\}$ sub-grids. Table 1 shows the corresponding number of local/global decision variables n_x/n_y , the number of local equality/inequality constraints n_e/n_i , and the number of global equality/inequality constraints n_{ey}/n_{iy} . We employ ADMM from [37] with penalty parameters $\rho \in \{10^0, 10^1, 10^2, 10^3\}$.

Figure 4a illustrates the numerical performance of both primal decomposition variants and ADMM for the HVAC problems. Figure 5 shows their performance for the OPF problems. Figure 4b shows the AL formulation only, since the ℓ_1 formulation runs out

⁶Note that the proposed framework is flexible with respect to the interior point solvers used in the subproblems as long as one can access the corresponding sensitivity matrices.

of memory for this problem. The constraint violations for the equality constraints (1b), $\| [A^x \ A^y] [x^\top \ y^\top]^\top - b \|_\infty$, for the inequality constraints (1c), $\max([B^x \ B^y] [x^\top \ y^\top]^\top - b)$, and the value of the cost function $f([x^\top, y^\top]^\top)$ from (1a) are displayed, where the x-axis shows the iteration count. One can observe that the primal decomposition schemes achieve a high degree of feasibility in less than 10 iterations for all cases. Moreover, the optimality gap $(f([x^\top, y^\top]^\top) - f([x^{\star\top}, y^{\star\top}]^\top)) / f([x^{\star\top}, y^{\star\top}]^\top)$ is below 0.01% in less than 10 iterations for both primal decomposition variants and for all $|\mathcal{S}|$, where $[x^{\star\top}, y^{\star\top}]^\top$ is computed via **Ipopt**. For ADMM, infeasibility and the optimality gap stay large independently of the choice of ρ .

Remark 3 (Scaling of the ℓ_1 formulation). *The reason for the poor scaling of the ℓ_1 -formulation is two-fold: First, the relaxation (8) introduces $2n_y$ additional slack variables and inequality constraints. Hence, the KKT system in the subproblems defined via (26) has a larger size than the KKT system we get with the AL formulation (24). Moreover, the additional inequality constraints potentially lead to smaller stepsizes due to the fraction-to-boundary rule [30, Eq 19.9]. Hence, more iterations in the subproblems are required compared to the AL formulation.*

8. Discussion of Algorithmic Properties

Next, we discuss algorithm properties in view of the desirable properties from Section 1.

Computation Times

Comparing computation times between algorithms is difficult, since the numerical performance strongly depends on the implementation. Nonetheless, we would like to provide some timing information to underline the potential of primal decomposition methods. Table 2 shows the computation times and the number of iterations for all algorithms. **Ipopt** is terminated at optimality with default settings and the computation time for the primal decomposition schemes are evaluated once an optimality gap of 10^{-4} and a maximum constraint violation for equality/inequality constraints of 10^{-5} is reached. ADMM is terminated after a maximum of 5,000 iterations. One can observe that the AL formulation and **Ipopt** have similar computation times independently of $|\mathcal{S}|$. Although fast computation is not our primary focus, this indicates the potential of primal decomposition for large-scale optimization.

Both, ADMM and the open-source solver **OSQP** are not able to solve the HVAC problems to a sufficient accuracy with a reasonable number of iterations (4,000 for **OSQP** and 5,000 for ADMM). This indicates that these problems are rather challenging, which might be due to the large number of inequality constraints coming from the temperature bounds. The computation time of ADMM, however, remains reasonable even for 5,000 iterations since we use warm-started **OSQP** as a very fast local solver parallelized via multi-threading. In case less-strict termination tolerances are required, ADMM might become as fast as primal decomposition, overall. Both primal decomposition schemes require far less iterations. **Ipopt** requires more than 100 iterations, which is unusual for

Table 2: Timing and number of iterations for the HVAC and the OPF problem with $|\mathcal{S}| \in \{30, 180, 300\}$ buildings and $|\mathcal{S}| \in \{29, 64\}$ sub-grids, 30 cores.

	$ \mathcal{S} $		AL	$l1$	Ipopt	ADMM	ADMM
					par. LA	$\rho = 10$	$\rho = 100$
HVAC	300	t[s]	431.5	-	386.7	892.8*	1,122.2*
	180		195.7	-	218.1	510.3*	1,322.2*
	30		18.1	270.0	25.5	72.8*	85.53*
OPF	64	t[s]	2.64	283.89	4.64	70.52*	111.29*
	29		1.83	95.76	2.01	13.54	61.58*
HVAC	300	iter.	13	-	145	5,000*	5,000*
	180		12	-	141	5,000*	5,000*
	30		13	12	104	5,000*	5,000*
OPF	64	iter.	9	9	16	3,199*	5,000*
	29		9	7	15	1,133	5,000*
term.			rel. opt.	10^{-4}	optimal	rel. opt.	10^{-4}
			infeas.	10^{-5}		infeas.	10^{-5}

*terminated because max. iterations reached.

Table 3: Internal timing (%) for the AL formulation and the HVAC problem, 30 cores.

$ \mathcal{S} $	sensitivity eval.	local sol.	coord.	line search	other
300	68.10	6.66	6.10	17.84	1.30
180	41.58	19.86	9.02	26.89	2.65
30	4.37	6.69	9.35	79.29	0.30

interior-point methods. A possible explanation is that interior-point methods typically choose the smallest stepsize such that no inequality constraint is violated (fraction-to-boundary rule) [30, Eq 19.9]. This can lead to a slow progress since in this case only small steps are taken. Primal decomposition mitigates this, since each subproblem has its “own” stepsize when solving the subproblems.

For the OPF problems (18), computation times are generally lower because of smaller problem dimensions, cf. Table 1. The qualitative performance of all algorithms relative to each other is similar to what we have observed for the HVAC problems.

Internal timings for the AL formulation and different sizes $|\mathcal{S}|$ for the HVAC problem are shown in Table 3. Here, the time spent in the coordination problem (13) and in the local solvers stays relatively constant for varying $|\mathcal{S}|$. The time spent for sensitivity computation, however, increases significantly with $|\mathcal{S}|$. One explanation for that is that the complexity in the backsolves for computing the Hessian via (12) increases with $O(n_y^3)$. In case the backsolves can be parallelized, for example if the subproblems themselves use multi-threading in a cluster environment, computation time can be reduced.

Table 4: Properties of ADMM and Primal Decomposition.

		ADMM	Primal Decomp.
Communication (#floats step)	forward	$\mathcal{O}(n_y)$	$\mathcal{O}((N_{ls} + 1)n_y)$
	backward	$\mathcal{O}(n_y)$	$\mathcal{O}((n_y^i)^2 + n_y)$
Computation	local	Convex QP	NLP
	global	Convex QP	NLP + lin. equations with multiple rhs.
Conv. rate (max.)		Linear	(Superlinear) [#]
Decentralization		Decentralized*	Distributed

*in the sense that decentralization of ADMM is straight-forward.

[#]to a solution of the barrier problem (5)

Feasibility and Optimality

Reaching feasibility fast is often crucial in the context of infrastructure systems to ensure system stability. Here, primal decomposition can shine. For all case studies, one can observe a high degree of primal feasibility in 10-20 iterations. ADMM requires far more iterations to reach a sufficient degree of feasibility, which is a known limitation of ADMM [4].

Communication

Primal decomposition (Algorithm 4) requires communication of the current iterate y^k to all subsystems $\mathcal{O}(N_{ls} + 1)$ times, where N_{ls} is the number of line search steps. For backward communication, both primal decomposition schemes require the gradient $g_i \doteq \nabla_y \phi_i$ and the Hessian $H_i \doteq \nabla_{yy}^2 \phi_i$ of the optimal value functions once in each outer iteration from the subsystems to the master. The communication of the Hessian is the most expensive step, but the H_i are typically highly sparse and symmetric, which reduces its communication demand. Figure 6 exemplarily shows the sparsity pattern of the Hessian of the second subsystem $H_2 = \nabla_{yy}^2 \phi_2(y)$ for one HVAC and one OPF problem. For OPF, H_2 is diagonal and thus very cheap to communicate. For HVAC, H_2 is almost diagonal except for one dense block. This comes from the fact that the local Hessians $\{H_i\}_{i \in \mathcal{S}}$ have non-zero entries only for the coupling elements of y to the i th subsystem plus the non-zero entries in H_i^{yy} cf. (22). We denote by n_y^i the number of coupling variables between the i th subsystem and the master in the following. For the OPF problems, the subsystems are coupled to the master only via one bus of active power exchange, which leads to a $(1, 1)$ -Hessian block and thus H_2 is diagonal. Similarly for the HVAC problems, the subproblems are coupled to the master via power exchange occurring over 24 time steps, which leads to a dense $(24, 24)$ -Hessian block. Thus, each subsystem $i \in \mathcal{S}$ needs to communicate $\mathcal{O}(n_y^i(n_y^i + 1)/2 + n_y + N_{ls}^k + 1)$ floats to the master taking the Hessian's symmetry and communication of g_i and $\phi_i(y^k)$ for each line search step into account.

ADMM requires to communicate y^k from the master to all subproblems and the corresponding local equivalent z_i^k from all subsystems to the master in each iteration [37]. Hence, forward and backward communication is $\mathcal{O}(n_y)$.

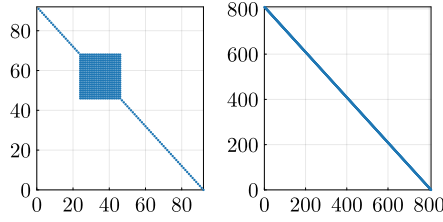


Figure 6: Sparsity patterns of $\nabla_{yy}^2 \phi_2(y)$ for the HVAC problem with $|\mathcal{S}| = 4$ (left) and the OPF problem with $|\mathcal{S}| = 29$ (right).

Figure 7 shows the forward and backward communication for AL-based primal decomposition and ADMM for the HVAC problem with $|\mathcal{S}| = 30$, and for the OPF problem with $|\mathcal{S}| = 39$ for one subsystem. One can see that for the HVAC problem, AL’s backward communication is approximately twice the ADMM communication as we have to communicate the dense Hessian block. However, since $n_i^y \ll n_y$, the difference remains small. In later iterations, forward communication increases due to a higher number of line search steps.

For the OPF problem, the forward communication costs of primal decomposition and ADMM are similar since no line search is required. Backward communication is twice as high in primal decomposition because of the diagonal Hessian.

Decentralization

If decentralization is required, i.e. avoiding central coordination, ADMM is advantageous since decentralization is straight-forward. Important properties of primal decomposition and ADMM are summarized in Table 4.

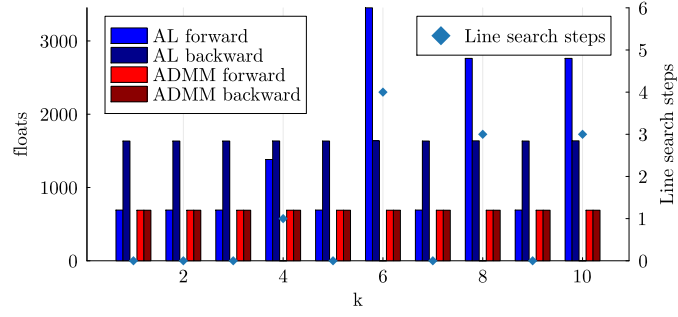
9. Conclusion and Outlook

We have presented two primal decomposition schemes to solve large-scale QPs for the operation of infrastructure networks. The developed methods are proven to converge globally to the optimal solution. Numerical experiments have demonstrated their potential for solving large-scale QPs in a small number of iterations to a high degree of feasibility and optimality, which distinguishes them from classical distributed methods such as ADMM. Moreover, we have shown that primal decomposition based on augmented Lagrangians has numerical benefits compared to the classical ℓ_1 -formulation.

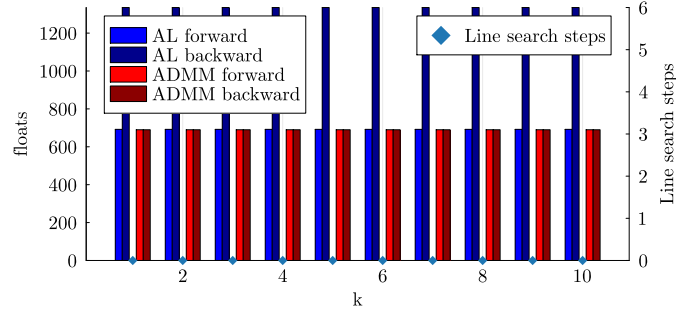
Future work will further improve implementation aspects of the developed primal decompositions schemes. Sparse backsolves or quasi-Newton Hessian approximations have the potential to greatly accelerate Hessian computation.

A. Sensitivities for Augmented Lagrangians

Observe that for computing $\nabla_y \Phi_i^\delta$ and $\nabla_{yy}^2 \Phi_i^\delta$ in (10) and (11), the partial derivatives of the implicit function F_i^δ and L_i are required. Next, we derive these quantities for the



(a) HVAC problem with $|\mathcal{S}| = 30$.



(b) OPF problem with $|\mathcal{S}| = 29$.

Figure 7: Communication (#floats) for one subsystem.

two relaxed local problems (6) and (8).

For (6), the Lagrangian (omitting arguments) reads

$$\begin{aligned} L_i^{\delta, \rho} \doteq & \frac{1}{2} \begin{bmatrix} x_i \\ y \\ z_i \end{bmatrix}^\top \begin{bmatrix} H_i^{xx} & H_i^{xy} & 0 \\ H_i^{xy\top} & H_i^{yy} + \rho I & -\rho I \\ 0 & -\rho I & \rho I \end{bmatrix} \begin{bmatrix} x_i \\ y \\ z_i \end{bmatrix} + \begin{bmatrix} h_i^x \\ h_i^y + \lambda_i^k \\ -\lambda_i^k \end{bmatrix}^\top \begin{bmatrix} x_i \\ y \\ z_i \end{bmatrix} \\ & - \delta \mathbf{1}^\top \ln(s_i) + \gamma_i^\top \left([A_i^x \ A_i^y] [x_i^\top \ z_i^\top]^\top - b_i \right) \\ & + \mu_i^\top ([B_i^x \ B_i^y] [x_i^\top \ z_i^\top]^\top + s_i - d_i). \end{aligned}$$

Hence, the local KKT conditions read

$$T_i^{\delta, \rho}(q_i^*, y) \doteq \begin{bmatrix} H_i^{xx} x_i^* + H_i^{xy} y + h_i^x + A_i^{x\top} \gamma_i^* + B_i^{x\top} \mu_i^* \\ \rho(z_i^* - y) - \lambda_i^k + A_i^{y\top} \gamma_i^* + B_i^{y\top} \mu_i^* \\ -(S_i^*)^{-1} \delta \mathbf{1} + \mu_i^* \\ [A_i^x \ A_i^y] [x_i^{*\top} \ z_i^{*\top}]^\top - b_i \\ [B_i^x \ B_i^y] [x_i^{*\top} \ z_i^{*\top}]^\top + s_i^* - d_i \end{bmatrix} = 0,$$

where $q_i^\top \doteq [x_i^\top, z_i^\top, s_i^\top, \gamma_i^\top, \mu_i^\top]$. Moreover,

$$\nabla_{q_i} T_i^{\delta, \rho}(q_i, y) = \begin{bmatrix} H_i^{xx} & 0 & 0 & A_i^{x\top} & B_i^{x\top} \\ 0 & \rho I & 0 & A_i^{y\top} & B_i^{y\top} \\ 0 & 0 & S_i^{-1} M_i & 0 & I \\ A_i^x & A_i^y & 0 & 0 & 0 \\ B_i^x & B_i^y & I & 0 & 0 \end{bmatrix}, \quad (20)$$

$$\nabla_y T_i^{\delta, \rho}(q_i, y) = [H_i^{xy\top} \ -\rho I \ 0 \ 0 \ 0]^\top, \quad (21)$$

where $M_i = \text{diag}(\mu_i)$. Moreover, by (10), $\nabla_y \Phi_i^{\delta, \rho}(y) = \nabla_y L_i^{\delta, \rho}(q_i^*(y); y) = (H_i^{yy} + \rho I)y + H_i^{xy} x_i^* + h_i^y + \lambda_i^k - \rho z_i^*$. Furthermore, by (11),

$$\nabla_{yy}^2 \Phi_i^{\delta, \rho}(y) = H_i^{yy} + \rho I + [H_i^{xy\top} \ -\rho I \ 0 \ 0 \ 0] \nabla_y q_i^*(y), \quad (22)$$

where $q_i^*(y)$ is computed by the system of linear equations

$$\nabla_{q_i} T_i^{\delta, \rho}(q_i^*, y) \nabla_y q_i^*(y) = -\nabla_y T_i^{\delta, \rho}(q_i^*, y) \quad (23)$$

Precomputation for Hessian Evaluation

Next, we show how to precompute matrices to make (23) easier to solve, cf. [39, Sec IV]. We assume that H_i^{xx} is invertible—if this is not the case, one can use the variant without precomputation. Recall that by (22), we need to compute $H_i^{xy\top} \nabla_y x_i^* - \rho \nabla_y z_i^*$,

where $(\nabla_y x_i^*, \nabla_y z_i^*)$ are given by (23):

$$\begin{bmatrix} H_i^{xx} & 0 & 0 & A_i^{x\top} & B_i^{x\top} \\ 0 & \rho I & 0 & A_i^{y\top} & B_i^{y\top} \\ 0 & 0 & S_i^{\star-1} M_i^{\star} & 0 & I \\ A_i^x & A_i^y & 0 & 0 & 0 \\ B_i^x & B_i^y & I & 0 & 0 \end{bmatrix} \begin{bmatrix} \nabla_y x_i^* \\ \nabla_y z_i^* \\ \nabla_y s_i^* \\ \nabla_y \gamma_i^* \\ \nabla_y \mu_i^* \end{bmatrix} = \begin{bmatrix} -H_i^{xy} \\ \rho I \\ 0 \\ 0 \\ 0 \end{bmatrix}. \quad (24)$$

By the third block-row, we have that $\nabla_y s_i^* = -M_i^{\star-1} S_i^{\star} \nabla_y \mu_i^*$. This yields

$$\begin{bmatrix} H_i^{xx} & 0 & A_i^{x\top} & B_i^{x\top} \\ 0 & \rho I & A_i^{y\top} & B_i^{y\top} \\ A_i^x & A_i^y & 0 & 0 \\ B_i^x & B_i^y & 0 & -M_i^{\star-1} S_i^{\star} \end{bmatrix} \begin{bmatrix} \nabla_y x_i^* \\ \nabla_y z_i^* \\ \nabla_y \gamma_i^* \\ \nabla_y \mu_i^* \end{bmatrix} = \begin{bmatrix} -H_i^{xy} \\ \rho I \\ 0 \\ 0 \end{bmatrix}.$$

Since H_i^{xx} is invertible, we have

$$\begin{bmatrix} \nabla_y x_i^* \\ \nabla_y z_i^* \end{bmatrix} = \underbrace{\begin{bmatrix} H_i^{xx} & 0 \\ 0 & \rho I \end{bmatrix}^{-1}}_{\doteq P_i^{-1}} \left[\begin{bmatrix} -H_i^{xy} \\ \rho I \end{bmatrix} - \underbrace{\begin{bmatrix} A_i^x & A_i^y \\ B_i^x & B_i^y \end{bmatrix}^{\top}}_{\doteq K_i^{\top}} \begin{bmatrix} \nabla_y \gamma_i^* \\ \nabla_y \mu_i^* \end{bmatrix} \right]. \quad (25)$$

Employing the Schur complement with respect to the first two block rows yields

$$\underbrace{\begin{bmatrix} K_i P_i^{-1} K_i^{\top} + \begin{bmatrix} 0 & 0 \\ 0 & M_i^{\star-1} S_i^{\star} \end{bmatrix} \end{bmatrix}}_{\doteq W_i} \begin{bmatrix} \nabla_y \gamma_i^* \\ \nabla_y \mu_i^* \end{bmatrix} = \underbrace{\begin{bmatrix} -A_i^x H_i^{xx-1} H_i^{xy} + A_i^y \\ B_i^x H_i^{xx-1} H_i^{xy} + B_i^y \end{bmatrix}}_{\doteq R_i}.$$

Observe that H_i^{xx-1}, K_i and R_i can be precomputed. Moreover, the above system of linear equations has significantly less decision variables compared to (23) and is in addition positive definite under Assumption 1. This allows to use the Cholesky or Bunch-Kaufmann (LDL) factorization instead of LU.

Sensitivities for the $\ell 1$ Formulation

The Lagrangian to (8) reads

$$\begin{aligned} L_i = & \frac{1}{2} \begin{bmatrix} x_i \\ z_i \end{bmatrix}^{\top} \begin{bmatrix} H_i^{xx} & H_i^{xy} \\ H_i^{xy\top} & H_i^{yy} \end{bmatrix} \begin{bmatrix} x_i \\ z_i \end{bmatrix} + \begin{bmatrix} h_i^x \\ h_i^y \end{bmatrix}^{\top} \begin{bmatrix} x_i \\ z_i \end{bmatrix} \\ & + \bar{\lambda} \mathbf{1}^{\top} (v_i + w_i) - \delta (\mathbf{1}^{\top} \ln(s_i) + \mathbf{1}^{\top} \ln(v_i) + \mathbf{1}^{\top} \ln(w_i)) \\ & + \chi_i^{\top} (y - z_i - v_i + w_i) + \gamma_i^{\top} \left(\begin{bmatrix} A_i^x & A_i^y \end{bmatrix} \begin{bmatrix} x_i^{\top} & z_i^{\top} \end{bmatrix}^{\top} - b_i \right) \\ & + \mu_i^{\top} \left(\begin{bmatrix} B_i^x & B_i^y \end{bmatrix} \begin{bmatrix} x_i^{\top} & z_i^{\top} \end{bmatrix}^{\top} + s_i - d_i \right). \end{aligned}$$

Hence, the KKT conditions require

$$T_i^{\delta, \bar{\lambda}}(u_i^*, y) \doteq \begin{bmatrix} H_i^{xx}x_i^* + H_i^{xy}z_i^* + h_i^x + A_i^{x\top}\gamma_i^* + B_i^{x\top}\mu_i^* \\ H_i^{yy}z_i^* + H_i^{xy\top}x_i^* + h_i^y - \chi_i^* + A_i^{y\top}\gamma_i^* + B_i^{y\top}\mu_i^* \\ -S_i^{-1}\delta\mathbf{1} + \mu_i^* \\ -\delta V_i^{-1}\mathbf{1} + (\bar{\lambda}\mathbf{1} - \chi_i^*) \\ -\delta W_i^{-1}\mathbf{1} + (\bar{\lambda}\mathbf{1} + \chi_i^*) \\ [A_i^x \ A_i^y] [x_i^{*\top} \ z_i^{*\top}]^\top - b_i \\ [B_i^x \ B_i^y] [x_i^{*\top} \ z_i^{*\top}]^\top + s_i^* - d_i \\ y - z_i^* - v_i^* + w_i^* \end{bmatrix} \stackrel{!}{=} 0,$$

where $u_i^\top \doteq [x_i^\top, z_i^\top, s_i^\top, v_i^\top, w_i^\top, \gamma_i^\top, \mu_i^\top, \chi_i^\top]$. Thus,

$$\nabla_{u_i} T_i^{\delta, \bar{\lambda}}(u_i, y) = \begin{bmatrix} H_i^{xx} & H_i^{xy} & 0 & 0 & 0 & A_i^{x\top} B_i^{x\top} & 0 \\ H_i^{xy\top} & H_i^{yy} & 0 & 0 & 0 & A_i^{y\top} B_i^{y\top} & -I \\ 0 & 0 & S_i^{-1} M_i & 0 & 0 & 0 & I \\ 0 & 0 & 0 & V_i^{-1}(\bar{\lambda}I - X_i) & 0 & 0 & -I \\ 0 & 0 & 0 & 0 & W_i^{-1}(\bar{\lambda}I + X_i) & 0 & I \\ A_i^x & A_i^y & 0 & 0 & 0 & 0 & 0 \\ B_i^x & B_i^y & I & 0 & 0 & 0 & 0 \\ 0 & -I & 0 & -I & I & 0 & 0 \end{bmatrix}, \quad (26)$$

where $V_i = \text{diag}(v_i)$, $W_i = \text{diag}(w_i)$, and $X_i = \text{diag}(\chi_i)$. Moreover,

$$\nabla_y T_i^{\delta, \bar{\lambda}}(u_i, y) = [0 \ 0 \ 0 \ 0 \ 0 \ 0 \ 0 \ I]^\top. \quad (27)$$

Furthermore, $\nabla_y \Phi_i^{\delta, \bar{\lambda}}(y) = \nabla_y L_i = \chi_i$, $\nabla_{yy} L_i = 0$, and $\nabla_{yu_i^*} L_i = [0 \ 0 \ 0 \ 0 \ 0 \ 0 \ 0 \ I]$. Thus, by (11),

$$\nabla_{yy} \Phi_i^{\delta, \bar{\lambda}}(y) = \nabla_y \chi_i^*(y). \quad (28)$$

B. Proof of Lemma 1

First, we will show that $Z^\top(ZCZ^\top)^{-1}Z = Z^\top ZC^{-1}Z^\top Z$ for a regular, symmetric $C \in \mathbb{R}^{n \times n}$, $Z \in \mathbb{R}^{m \times n}$ with $m < n$. Consider a re-ordered eigendecomposition $C = Q\Lambda Q^\top$ and partition $Q = [Q_1 \ Q_2]$, $\Lambda_i = \text{blkdiag}(\Lambda_1, \Lambda_2)$ such that Q_2 is a nullspace-basis of Z , i.e. $ZQ_2 = 0$. Hence, we have $ZCZ^\top = Z[Q_1 \ Q_2] \text{blkdiag}(\Lambda_1, \Lambda_2) [Q_1 \ Q_2]^\top Z^\top = ZQ_1\Lambda_1Q_1^\top Z^\top$ since $ZQ_2 = 0$. Thus, $Z^\top(ZCZ^\top)^{-1}Z = Z^\top ZQ_1\Lambda_1^{-1}Q_1^\top Z^\top Z$. Again, since $ZQ_2 = 0$, by expansion, $Z^\top Z[Q_1 \ Q_2] \text{blkdiag}(\Lambda_1^{-1}, \Lambda_2^{-1}) [Q_1 \ Q_2]^\top Z^\top Z = Z^\top ZC^{-1}Z^\top Z$.

Proof of a): By (22), we need $\nabla_y q_i^*(y)$ for computing $\nabla_{yy} \Phi_i^{\delta, \rho}$, where $\nabla_y q_i^*(y)$ is defined by (23). Define $C_i \doteq \text{blkdiag}(H_i^{xx}, \rho I, S_i^{-1} M_i)$, $D_i \doteq \begin{bmatrix} A_i^x & A_i^y & 0 \\ B_i^x & B_i^y & I \end{bmatrix}$, and $E_i \doteq [H_i^{xy\top} - \rho I \ 0]^\top$. Consider (21) and parametrize $(\nabla_y x_i^{*\top}, \nabla_y z_i^{*\top}, \nabla_y s_i^{*\top})^\top \doteq Z_i P_i$, where Z_i is a nullspace matrix to D_i , i.e., the columns of Z_i form an orthogonal basis of

the nullspace of D_i and $P_i \in \mathbb{R}^{(n_{x_i}+n_y-\text{nr}(A_i^x)) \times n_y}$ is an auxiliary matrix. Using the above parametrization in (23) and multiplying with Z_i^\top yields $Z_i^\top C_i Z_i P_i = -Z_i^\top E_i$ by $Z_i^\top D_i^\top = 0$. Since $s_i, \mu_i > 0$ and Assumption 1 holds, we have $C_i \succ 0$ and thus $Z_i^\top C_i Z_i$ is invertible by full rank of Z_i . Hence, by (22) and the above derivation, $\nabla_{yy} \Phi_i^{\delta, \rho}(y) = H_i^{yy} + \rho I - E_i^\top Z_i (Z_i^\top C_i Z_i)^{-1} Z_i^\top E_i = H_i^{yy} + \rho I - E_i^\top Z_i Z_i^\top C_i^{-1} Z_i Z_i^\top E_i$. Notice that $Z_i Z_i^\top$ is a diagonal matrix with $\text{rank}(Z_i)$ ones and $\dim(C_i) - \text{rank}(Z_i)$ zeros. Hence, since C_i is positive definite, it suffices to show that $\nabla_{yy} \Phi_i^{\delta, \rho}(y) \succ 0$ for the worst case, i.e. $Z_i Z_i^\top = I$ (no constraints). Thus, $\nabla_{yy} \Phi_i^{\delta, \rho}(y) = H_i^{yy} - H_i^{xy\top} (H_i^{xx})^{-1} H_i^{xy} \succ 0$ by the definition of E_i, C_i , by Assumption 1 a) and the Schur-complement Lemma [40, A.14].

Proof of b): By (28), we need to show that $\nabla_y \chi_i^*(y) \succ 0$, which can be computed by the system of linear equations (26), (27). Define $F_i = \text{blkdiag} \left(\begin{bmatrix} H_i^{xx} & H_i^{xy} \\ H_i^{xy\top} & H_i^{yy} \end{bmatrix}, S_i^{-1} M_i, V_i^{-1} (\bar{\lambda} - X_i), W_i^{-1} (\bar{\lambda} + X_i) \right)$ and $G_i \doteq \begin{bmatrix} A_i^x & A_i^y & 0 & 0 & 0 \\ B_i^x & B_i^y & I & 0 & 0 \\ 0 & -I & 0 & -I & I \end{bmatrix}$. By Assumption 1, $s_i, v_i, w_i, \mu_i >$

0, and $\bar{\lambda} > \max_j |[\chi_i]_j|$, we have that $F_i \succ 0$. Hence, $(\nabla_y x_i^{*\top}, \nabla_y z_i^{*\top}, \nabla_y s_i^{*\top}, \nabla_y v_i^{*\top}, \nabla_y w_i^{*\top})^\top = -F_i^{-1} G_i (\nabla_y \gamma_i^{*\top}, \nabla_y \mu_i^{*\top}, \nabla_y \chi_i^{*\top})$. Thus, $G_i^\top F_i^{-1} G_i (\nabla_y \gamma_i^{*\top}, \nabla_y \mu_i^{*\top}, \nabla_y \chi_i^{*\top}) = [0 \ 0 \ I]^\top$. Since $F_i^{-1} \succ 0$ and by full rank of G_i from Assumption 1, $G_i^\top F_i^{-1} G_i \succ 0$ and thus $(\nabla_y \gamma_i^{*\top}, \nabla_y \mu_i^{*\top}, \nabla_y \chi_i^{*\top}) = (G_i^\top F_i^{-1} G_i)^{-1} [0 \ 0 \ I]^\top$. Since $(G_i^\top F_i^{-1} G_i)^{-1} \succ 0$, all leading principle minors of this matrix must be positive definite by Sylvester's criterion [41, Col 7.1.5]. By variable reordering, the assertion follows.

C. Solution of (1) via ADMM

We derive a distributed ADMM version for (1) as a baseline for numerical comparison. Consider (1), introduce auxiliary variables $z_i \in \mathbb{R}^{n_y}$ and consensus constraints $y = z_1 = \dots = z_S \mid \lambda_1, \dots, \lambda_S$. This yields

$$\min_{x, y, z} \sum_{i \in \mathcal{S}} \frac{1}{2} \begin{bmatrix} x_i \\ z_i \end{bmatrix}^\top \begin{bmatrix} H_i^{xx} & H_i^{xy} \\ H_i^{xy\top} & H_i^{yy} \end{bmatrix} \begin{bmatrix} x_i \\ z_i \end{bmatrix} + \begin{bmatrix} h_i^x \\ h_i^y \end{bmatrix}^\top \begin{bmatrix} x_i \\ z_i \end{bmatrix} \quad (29a)$$

$$\text{subject to } \begin{bmatrix} A_i^x & A_i^y \end{bmatrix} \begin{bmatrix} x_i^\top & z_i^\top \end{bmatrix}^\top - b_i = 0, \quad i \in \mathcal{S}, \quad (29b)$$

$$\begin{bmatrix} B_i^x & B_i^y \end{bmatrix} \begin{bmatrix} x_i^\top & z_i^\top \end{bmatrix}^\top - d_i \leq 0, \quad i \in \mathcal{S}, \quad (29c)$$

$$A^y y - b^y = 0, \quad B^y y - d^y \leq 0 \quad (29d)$$

$$z_i = y, \quad i \in \mathcal{S}. \quad (29e)$$

The augmented Lagrangian with respect to $y - z_i = 0$ reads

$$L^\rho = \sum_{i \in \mathcal{S}} \phi_i^x(x_i, z_i) + \phi^y(y) + \lambda_i^{k\top} (y - z_i) + \frac{\rho}{2} \|y - z_i\|^2,$$

where ϕ_i^x are defined by (29a)-(29c) and ϕ^y is the indicator function for (29d). Minimizing L^ρ w.r.t. (x_i, z_i) for fixed (y^k, λ_i^k) yields for all $i \in \mathcal{S}$

$$\begin{aligned} (x_i^{k+1}, z_i^{k+1}) = \arg \min_{x_i, z_i} & \frac{1}{2} \begin{bmatrix} x_i \\ z_i \end{bmatrix}^\top \begin{bmatrix} H_i^{xx} & H_i^{xy} \\ H_i^{xy^\top} & H_i^{yy} + \rho I \end{bmatrix} \begin{bmatrix} x_i \\ z_i \end{bmatrix} + \begin{bmatrix} h_i^x \\ h_i^y - \lambda_i^k - \rho y^k \end{bmatrix}^\top \begin{bmatrix} x_i \\ z_i \end{bmatrix} \\ \text{subject to} & \quad \begin{bmatrix} A_i^x & A_i^y \end{bmatrix} \begin{bmatrix} x_i^\top & z_i^\top \end{bmatrix}^\top - b_i = 0, \\ & \quad \begin{bmatrix} B_i^x & B_i^y \end{bmatrix} \begin{bmatrix} x_i^\top & z_i^\top \end{bmatrix}^\top - d_i \leq 0. \end{aligned} \quad (30)$$

Minimising L^ρ w.r.t. y for fixed $(x_i^{k+1}, z_i^{k+1}, \lambda_i^k)$ yields

$$\begin{aligned} y^{k+1} = \arg \min_y & \sum_{i \in \mathcal{S}} \frac{\rho}{2} y^\top y + (\lambda_i^k - \rho z_i^{k+1})^\top y \\ \text{subject to} & \quad A^y y - b^y = 0, \quad B^y y - d^y \leq 0. \end{aligned} \quad (31)$$

Finally, the Lagrange multiplier update reads

$$\lambda_i^{k+1} = \lambda_i^k + \rho(y^{k+1} - z_i^{k+1}), \quad i \in \mathcal{S}. \quad (32)$$

The update rules (30)-(32) define the ADMM iterations. Note that (30) and (32) can be executed locally for all $i \in \mathcal{S}$, whereas (31) defines the global coordination step.

References

- [1] F. Capitanescu, "TSO-DSO interaction: Active distribution network power chart for TSO ancillary services provision," *Electric Power Systems Research*, vol. 163, pp. 226-230, 2018.
- [2] M. Kalantar-Neyestanaki, F. Sossan, M. Bozorg, and R. Cherkaoui, "Characterizing the Reserve Provision Capability Area of Active Distribution Networks: A Linear Robust Optimization Method," *IEEE Transactions on Smart Grid*, vol. 11, no. 3, pp. 2464-2475, 2020.
- [3] H. Everett, "Generalized Lagrange multiplier method for solving problems of optimum allocation of resources," *Operations research*, vol. 11, no. 3, pp. 399-417, 1963.
- [4] S. Boyd, N. Parikh, E. Chu, B. Peleato, *et al.*, "Distributed Optimization and Statistical Learning via the Alternating Direction Method of Multipliers," *Foundations and Trends® in Machine Learning*, vol. 3, no. 1, pp. 1-122, 2011.
- [5] A. Nedić, A. Olshevsky, and W. Shi, "Achieving Geometric Convergence for Distributed Optimization Over Time-Varying Graphs," *SIAM Journal on Optimization*, vol. 27, no. 4, pp. 2597-2633, 2017.
- [6] E. K. Ryu and W. Yin, *Large-Scale Convex Optimization: Algorithms & Analyses via Monotone Operators*. Cambridge: Cambridge University Press, 2022.

- [7] T. Erseghe, “Distributed Optimal Power Flow Using ADMM,” *IEEE Transactions on Power Systems*, vol. 29, no. 5, pp. 2370–2380, 2014.
- [8] B. Kim and R. Baldick, “A comparison of distributed optimal power flow algorithms,” *IEEE Transactions on Power Systems*, vol. 15, no. 2, pp. 599–604, 2000.
- [9] S. Shin, C. Coffrin, K. Sundar, and V. M. Zavala, “Graph-Based Modeling and Decomposition of Energy Infrastructures,” *IFAC-PapersOnLine*, vol. 54, no. 3, pp. 693–698, 2021.
- [10] J. Huang, Z. Li, and Q. H. Wu, “Coordinated dispatch of electric power and district heating networks: A decentralized solution using optimality condition decomposition,” *Applied Energy*, vol. 206, pp. 1508–1522, 2017.
- [11] Y. Cao, W. Wei, L. Wu, S. Mei, *et al.*, “Decentralized Operation of Interdependent Power Distribution Network and District Heating Network: A Market-Driven Approach,” *IEEE Transactions on Smart Grid*, vol. 10, no. 5, pp. 5374–5385, 2019.
- [12] B. Coulbeck, M. Brdyś, C. H. Orr, and J. P. Rance, “A hierarchical approach to optimized control of water distribution systems: Part I decomposition,” *Optimal Control Applications and Methods*, vol. 9, no. 1, pp. 51–61, 1988.
- [13] N. Chiang, C. G. Petra, and V. M. Zavala, “Structured nonconvex optimization of large-scale energy systems using PIPS-NLP,” in *2014 Power Systems Computation Conference*, 2014, pp. 1–7.
- [14] V. M. Zavala, C. D. Laird, and L. T. Biegler, “Interior-point decomposition approaches for parallel solution of large-scale nonlinear parameter estimation problems,” *Chemical Engineering Science*, vol. 63, no. 19, pp. 4834–4845, 2008.
- [15] D. K. Varvarezos, L. T. Biegler, and I. E. Grossmann, “Multiperiod design optimization with SQP decomposition,” *Computers & Chemical Engineering*, vol. 18, no. 7, pp. 579–595, 1994.
- [16] A. Engelmann, Y. Jiang, T. Mühlpfordt, B. Houska, *et al.*, “Toward Distributed OPF Using ALADIN,” *IEEE Transactions on Power Systems*, vol. 34, no. 1, pp. 584–594, 2019.
- [17] B. Houska, J. Frasch, and M. Diehl, “An Augmented Lagrangian Based Algorithm for Distributed NonConvex Optimization,” *SIAM Journal on Optimization*, vol. 26, no. 2, pp. 1101–1127, 2016.
- [18] A. Engelmann, Y. Jiang, B. Houska, and T. Faulwasser, “Decomposition of Non-convex Optimization via Bi-Level Distributed ALADIN,” *IEEE Transactions on Control of Network Systems*, vol. 7, no. 4, pp. 1848–1858, 2020.
- [19] A. Engelmann, G. Stomberg, and T. Faulwasser, “An essentially decentralized interior point method for control,” in *60th IEEE Conference on Decision and Control*, 2021, pp. 2414–2420.
- [20] G. Stomberg, A. Engelmann, and T. Faulwasser, “Decentralized non-convex optimization via bi-level SQP and ADMM,” *IEEE 61st Annual Conference on Decision and Control*, 2022. arXiv: 2204.08786.

- [21] A. M. Geoffrion, “Primal Resource-Directive Approaches for Optimizing Nonlinear Decomposable Systems,” *Operations Research*, vol. 18, no. 3, pp. 375–403, 1970.
- [22] V. DeMiguel and W. Murray, “A local convergence analysis of bilevel decomposition algorithms,” *Optimization and Engineering*, vol. 7, no. 2, pp. 99–133, 2006.
- [23] V. DeMiguel and F. J. Nogales, “On Decomposition Methods for a Class of Partially Separable Nonlinear Programs,” *Mathematics of Operations Research*, vol. 33, no. 1, pp. 119–139, 2008. JSTOR: 25151844.
- [24] V. M. Zavala, C. D. Laird, and L. T. Biegler, “A fast moving horizon estimation algorithm based on nonlinear programming sensitivity,” *Journal of Process Control*, vol. 18, no. 9, pp. 876–884, 2008.
- [25] N. Yoshio and L. T. Biegler, “A Nested Schur decomposition approach for multi-period optimization of chemical processes,” *Computers & Chemical Engineering*, vol. 155, p. 107509, 2021.
- [26] S. Tu, A. Wächter, and E. Wei, “A Two-Stage Decomposition Approach for AC Optimal Power Flow,” *IEEE Transactions on Power Systems*, vol. 36, no. 1, pp. 303–312, 2021.
- [27] C. G. Petra and I. Aravena, *Solving realistic security-constrained optimal power flow problems*, 2021. arXiv: 2110.01669.
- [28] F. E. Curtis, D. K. Molzahn, S. Tu, A. Wächter, *et al.*, *A Decomposition Algorithm for Large-Scale Security-Constrained AC Optimal Power Flow*, 2021. arXiv: 2110.01737.
- [29] D. P. Bertsekas, *Nonlinear Programming*. Athena Scientific, Belmont, 1999.
- [30] J. Nocedal and S. Wright, *Numerical Optimization*. Springer Science & Business Media, New York, 2006.
- [31] D. P. Bertsekas, *Constrained Optimization and Lagrange Multiplier Methods*. Academic Press, 1982.
- [32] A. Wächter and L. T. Biegler, “On the implementation of an interior-point filter line-search algorithm for large-scale nonlinear programming,” *Mathematical Programming*, vol. 106, no. 1, pp. 25–57, 2006.
- [33] R. H. Byrd, G. Liu, and J. Nocedal, *On the Local Behavior of an Interior Point Method for Nonlinear Programming*. 1998.
- [34] J. B. Rawlings, N. R. Patel, M. J. Risbeck, C. T. Maravelias, *et al.*, “Economic MPC and real-time decision making with application to large-scale HVAC energy systems,” *Computers & Chemical Engineering*, vol. 114, pp. 89–98, 2018.
- [35] D. K. Molzahn and I. A. Hiskens, “A Survey of Relaxations and Approximations of the Power Flow Equations,” *Foundations and Trends® in Electric Energy Systems*, vol. 4, no. 1-2, pp. 1–221, 2019.

- [36] R. D. Zimmerman, C. E. Murillo-Sanchez, and R. J. Thomas, “MATPOWER: Steady-State Operations, Planning, and Analysis Tools for Power Systems Research and Education,” *IEEE Transactions on Power Systems*, vol. 26, no. 1, pp. 12–19, 2011.
- [37] A. Engelmann, S. Shin, F. Pacaud, and V. M. Zavala, *Scalable Primal Decomposition Schemes for Large-Scale Infrastructure Networks*, 2022. arXiv: 2212.11571.
- [38] B. Stellato, G. Banjac, P. Goulart, A. Bemporad, *et al.*, “OSQP: An operator splitting solver for quadratic programs,” *Mathematical Programming Computation*, 2020.
- [39] F. Pacaud, D. A. Maldonado, S. Shin, M. Schanen, *et al.*, “A feasible reduced space method for real-time optimal power flow,” *Electric Power Systems Research*, vol. 212, p. 108 268, 2022.
- [40] S. Boyd and L. Vandenberghe, *Convex Optimization*. Cambridge University Press, 2004.
- [41] R. A. Horn and C. R. Johnson, *Matrix Analysis*, 2nd edition. Cambridge University Press, 2013.